Egypt. J. Chem. **Vol. 68,** SI: Z. M. Nofal, pp. 237 - 253 (2025)

Egyptian Journal of Chemistry

http://ejchem.journals.ekb.eg/

Modification of Polysulfone Membrane with Green Synthesized Silica-Titanium (Si-TiO2) and Silica-Zinc (Si-ZnO) Nanocomposites for Environmental Applications

Abdulaziz F Sadik[1]*, Eman M. Mostafa[2] and Rabab M. El-Sherif [3]

[1]Faculty of Postgraduate Studies for Nanotechnology, Cairo University, El-Sheikh Zayed, 12588, Giza, Egypt; [2]PVT Lab., Production Department, Egyptian Petroleum Research Institute (EPRI), Cairo, (11727), Egypt, Faculty of Postgraduate Studies for Nanotechnology, Cairo University, El-Sheikh Zayed, 12588, Giza, Egypt; [3]Dean of the Faculty of Postgraduate Studies for Nanotechnology, Cairo University, El-Sheikh Zayed, 12588, Giza, Egypt;

Abstract

Desalination has emerged as a crucial solution to the growing demand for water, particularly in water-stressed nations, where desalination produces significantly more water than freshwater supplies. This study investigates the synthesis and characterization of novel metal-doped silica nanocomposite polysulfone (PSU) membranes to enhance their desalination performance. Green synthesis of PSU-Silica-Titanium and PSU-Silica-Zinc membranes. Qusing citrus peel extract was conducted. The membranes were characterized using X-ray diffraction (XRD), Raman spectroscopy, Brunauer-Emmett-Teller (BET) analysis, dynamic light scattering (DLS), zeta potential measurements, SEM-EDX, and transmission electron microscopy (TEM). Antimicrobial tests and quartz crystal microbalance (QCM) techniques were employed to evaluate the performance and salt rejection of the membranes. The presence of titanium and zinc oxide was confirmed by XRD, which showed a broad peak, suggesting the amorphous nature of PSU. Raman spectroscopy showed that the PSU structure was maintained. BET analysis revealed that the Si-TiO2 membrane had a larger pore volume and a lower surface area (0.10564 m^2/g) than the Si-ZnO membrane (0.03283 m^2/g). The DLS results indicated a smaller particle size for Si-TiO2 compared to Si-ZnO. The SEM-EDX results suggested greater aggregation in the Si-ZnO nanocomposite. The PSU- Si-TiO2 nanoparticles were spherical (20–50 nm) in the TEM images, whereas the PSU- Si-ZnO nanoparticles were irregular (30–80 nm). PSU-Si-TiO2 exhibited superior antimicrobial activity. Antimicrobial testing showed significant activity against microorganisms, although the PSU-Si-ZnO membranes had lower MIC and MBC values against *E. coli*, indicating their potential for both antimicrobial and anti-biofouling applications. The PSU-Si-TiO2 membrane demonstrated a good mix of stability (-0.53 Hz/min change) and salt rejection (1.02 μg/cm^2 adsorption), according to the QCM analysis. Despite certain improvements, the PSU-Si-ZnO membrane may have long-term challenges. In conclusion, both membranes exhibited high salt adsorption capacities, indicating their potential for specific ion removal, but may require further optimization for broader desalination applications.

Keywords: Polysulfone membrane; Nanocomposite; Water desalination; Titanium Nanocomposite; Zinc Nanocomposite; Silica nanoparticles.

1. Introduction

With advancements in science and technology, biomedicine, particularly in biomedical materials, has experienced rapid growth. Achieving low toxicity and excellent biocompatibility remains critical in developing these materials[1,2].

Seawater desalination has emerged as a promising strategy for addressing the global water crisis, particularly in water-scarce regions. It is a reliable alternative to traditional freshwater sources. Recent advancements in modern desalination technologies, particularly reverse osmosis (RO) and multi-stage flash distillation (MSF), have significantly improved their efficiency and reduced costs. These developments have made desalination an increasingly viable option for addressing global water scarcity [3,4]. However, desalination is energy-intensive, potentially contributing to greenhouse gas emissions if powered by fossil fuels [4]. Research has focused on improving membrane technology, which is an essential part of many desalination processes [5–7]. The salinity of the feed water, desired water quality, cost and availability of energy, environmental considerations, and intended use of the desalinated water all influence the choice of desalination method [8].

Polymeric membranes, such as polysulfone (PSU), have emerged as popular polymers for membrane fabrication in water desalination applications. They possess excellent physicochemical properties, remarkable thermal stability, strong

*Corresponding author e-mail: *abdulazizfsadik@gmail.com*.; (**Abdulaziz F Sadik**).
Received date 06 March 2025; Revised date 06 April 2025; Accepted date 13 May 2025
DOI: 10.21608/EJCHEM.2025.365900.11406
©2025 National Information and Documentation Center (NIDOC)

chemical resistance to various substances, including bases, acids, and chlorine, sufficient mechanical strength, and are suitable for large-scale production [9,10]. However, PSU membranes face challenges such as membrane fouling and wetting, which are two primary concerns. These issues have spurred extensive research into PSU membrane modifications to enhance their properties and overcome their inherent limitations [11].

Recent advancements in the modification of PSU membranes have focused on incorporating nanoparticles to enhance desalination efficiency. Researchers have explored the use of carbon nanotubes, silica nanoparticles, metal oxides, and nanocomposites for their potential to improve membrane properties [7,12,13]. Integrating nanocomposites into polymeric membranes has revolutionized membrane technology, significantly enhancing their performance and expanding their applications in various fields, such as water purification, gas separation, and biomedical sciences. This synergistic combination of nanomaterials and polymers leads to superior performance characteristics and addresses many of the limitations associated with conventional polymeric membranes [14].

Recent studies have investigated the incorporation of additives to improve membrane performance [15]. One study specifically focused on the fabrication of composite microfiltration membranes using a commercially available PSU polymer, incorporating polyethylene glycol (PEG) and sodium alginate (SA) through a non-solvent-induced phase separation (NIPS) method [16]. The results revealed that PEG-modified membranes exhibited higher porosity and flux than those modified with SA, demonstrating PEG's effectiveness of PEG as a pore-forming agent. In contrast, the SA-blended membranes exhibited lower contact angles, indicating higher hydrophilicity. These findings underscore how the introduction of additives can significantly alter the membrane structure and morphology, enhancing the porosity and tailoring the surface properties [17].

A recent study reported the development of a novel PSU ultrafiltration membrane designed for wastewater treatment using the (NIPS) technique. In this study, we incorporated a zinc ferrate-reduced graphene oxide (ZnFe2O4-rGO) nanocomposite as a modifier. They found that at an optimal concentration of 0.1 % w/v, the modified membrane significantly enhanced its hydrophilicity, permeability, and antifouling properties. This study demonstrates the potential of nanocomposite additives to improve PSU membrane performance [18]. A study investigated the production of three membranes with varying proportions of molybdenum sulfide (MoS_2) nanopowder. The effectiveness of these membranes improved with increased water permeability, while maintaining excellent salt retention. Various characterization methods were employed to evaluate the membranes, including scanning electron microscopy (SEM), Brunauer-Emmett-Teller (BET) analysis, and zeta potential measurements. The water permeability of the polyamide membrane containing 0.015% w/v PA-MoS_2 was measured at 29.79 $L/m^2 \cdot h \cdot bar$, which was significantly higher than that of the membranes with 0.005% w/v (19.36 $L/m^2 \cdot h \cdot bar$) and 0.01% w/v (3.63 $L/m^2 \cdot h \cdot bar$) PA-MoS_2. Under the same conditions, the membranes demonstrated salt rejection rates exceeding 96.0% for NaCl and 97.0% for $MgSO_4$. SEM analysis indicated that the 0.015% PA-MoS_2 membrane exhibited lower surface roughness, greater hydrophobicity, and higher water contact angle. However, due to the hydrophobic nature of MoS_2, these properties contributed to its lower salt rejection capabilities, greater hydrophobicity, and higher water contact angle. However, due to the hydrophobic nature of MoS_2, these properties contributed to its lower salt rejection capabilities [19].

A study investigated the preparation of a Polysulfone-Polyethylene Glycol (PS/PEG) flat sheet membrane using the phase inversion technique, with Dimethyl Formamide (DMF) as the solvent and deionized water as the coagulant. Different amounts of Polyethylene Glycol (PEG) were incorporated as polymeric improvers and pore-forming agents. To enhance the membrane performance, various nanoparticles have been incorporated, including single-walled carbon nanotubes (SWCNTs), multi-walled carbon nanotubes (MWCNTs), aluminum oxide (Al_2O_3), and copper oxide (CuO). The membranes, including neat PS, PS/PEG, and nanocomposite-modified membranes (M1, M2, M3, and M4), were characterized using Fourier-transform infrared spectroscopy (FTIR), scanning electron microscopy (SEM), and dynamic mechanical analysis (DMA). Their efficiency was evaluated using an Enhanced Direct Contact Membrane Distillation (EDCMD) unit, testing synthetic and saline water samples at a feed temperature of 60 °C. The membranes demonstrated a high salt rejection rate of 99.99%, with the maximum permeate flux observed in the following order: SWCNTs (20.91 $L/m^2 \cdot h$) >Al_2O_3 (19.92 $L/m^2 \cdot h$) >CuO (18.92 $L/m^2 \cdot h$) > MWCNTs (18.20 $L/m^2 \cdot h$). The optimal conditions for the process included feed and permeate temperatures of 60°C and 20°C, respectively. The PS/PEG/SWCNT membrane, which contained 0.5 wt.% SWCNTs exhibited a flux of 5.97 $L/m^2 \cdot h$ and demonstrated stable performance over 480 minutes of continuous desalination testing. This indicates the promising potential of the PS/PEG/SWCNT-modified membrane for water desalination applications using EDCMD [20]. Overall, previous studies suggest that various methods can enhance polysulfone (PSU) membranes, with each enhancement affecting properties such as hydrophilicity, salt rejection, water flux, or durability in different ways.

This study aimed to develop and characterize a novel nanocomposite polysulfone (PSU) membrane with enhanced desalination and antimicrobial properties through the synthesis of Silica-metal oxides *in situ* instead of preparing every nanoparticle alone then adding them to the membrane. Using a casting method, distinct PSU-based membranes were created, each modified with silica-based nanocomposites containing titanium and zinc, which imparted specific functionalities to the PSU base. Polysulfone was selected for its excellent mechanical strength, thermal stability, and chemical resistance.

The study is focused on improving the performance of membranes in specific filtration and separation processes, such as removing salt from seawater to produce freshwater in addition to enhancing antifouling and selectivity.

This study utilized advanced analytical techniques to characterize these membranes, employing nanocomposites synthesized from citrus peels to minimize the use of harmful chemicals. Key analytical methods included X-ray Diffraction (XRD) for assessing the crystalline structure, Raman spectroscopy for investigating molecular interactions, and Brunauer-Emmett-Teller (BET) analysis for evaluating the surface area and porosity. Dynamic Light Scattering (DLS) will be used to measure the particle size distribution, while zeta potential analysis will be used to assess the stability of the membranes in aqueous environments. Additionally, Scanning Electron Microscopy with Energy-Dispersive X-ray Spectroscopy (SEM-EDX) will provide insights into membrane morphology, and Transmission Electron Microscopy (TEM) will visualize the distribution of nanocomposites. To evaluate practical performance, salt rejection and antibiofouling activity were measured

using Quartz Crystal Microbalance (QCM) techniques and antimicrobial tests, respectively. This comprehensive approach aims to clarify the relationship between the structure, properties, and performance of these innovative PSU membranes, contributing to the development of more efficient and fouling-resistant membranes for desalination applications.

2. Results and Discussion

2.1. X-ray diffraction and Spectroscopy Analysis

The XRD patterns of both samples, PSU-Si-TiO2 and Si-ZnO PSU membranes (Figure 1), provide valuable information about their crystalline structure and composition. The membranes exhibited a characteristic broad peak centered at approximately 18-20°, indicating the amorphous nature of the polysulfone (PSU) polymer matrix. This standard feature confirmed the presence of PSU as the base material in all membranes [21]. The Si-TiO2 PSU membrane exhibited additional sharp peaks at 25.3°, 37.8°, and 48.0°, which can be attributed to titanium dioxide (TiO2) in its anatase phase. These peaks confirmed the successful incorporation of Ti into the PSU membrane. The sharpness of these peaks indicates the crystalline nature of the TiO2 particles, suggesting well-formed nanostructures within the polymer matrix [22,23]. In the case of the PSU-Si-ZnO membrane, distinct peaks were observed at 31.8°, 34.4°, and 36.3°. These peaks correspond to the (100), (002), and (101) planes of hexagonal wurtzite ZnO, respectively [24]. The presence of these peaks confirmed the incorporation of ZnO oxide nanoparticles into the membrane. The relatively high intensity of these peaks indicates good dispersion of ZnO within the PSU matrix, which could potentially enhance the functional properties of the membrane [25]. The differences in the peak intensities and positions among the samples indicate varying degrees of crystallinity and particle sizes of the incorporated metals. The sharp peaks in the Ti and ZnO-containing membranes suggest the formation of crystalline nanoparticles within the polymer matrix, which can potentially enhance the functional properties of these membranes for various applications, such as water purification and antimicrobial activity.

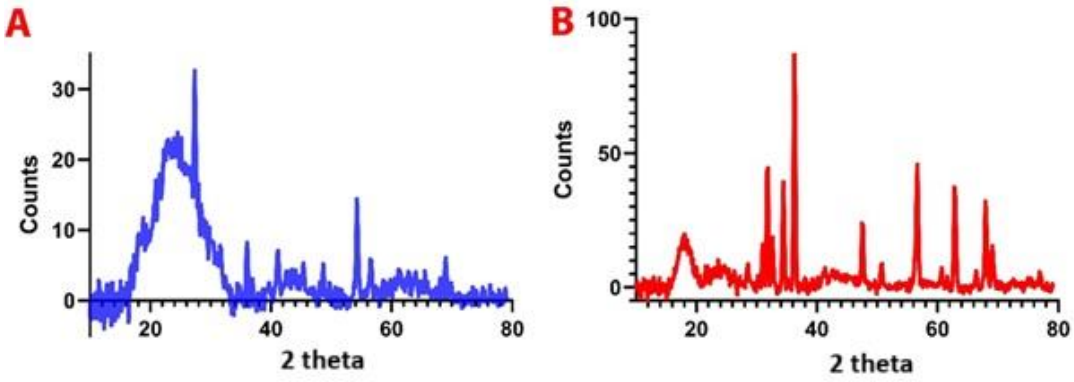

Figure 1 XRD patterns of both samples (A is PSU-Si-TiO2 and B is PSU-Si-ZnO)

Raman and Fourier-transform infrared spectroscopy were employed to analyze the structural characteristics of both nanocomposite polysulfone (PSU) membranes: Si-TiO2 and Si-ZnO. The Raman spectra provide valuable insights into the molecular structure, interactions, and potential modifications induced by incorporating different nanoparticles into PSU matrices. Both samples exhibited characteristic peaks associated with the PSU matrix, indicating that the fundamental polymer structure was preserved in both nanocomposite membranes. Figures 2 and 3 show that the key PSU peaks observed include (790-800 cm^{-1}: Symmetric C-S-C stretching), (1070-1080 cm^{-1}: Symmetric O=S=O stretching), (1110-1120 cm^{-1}: Asymmetric O=S=O stretching) and (1150-1160 cm^{-1}: C-O-C symmetric stretching) [3,4]. These peaks confirmed the presence of sulfone and ether groups, which are typical of PSU. The presence of silica nanoparticles in both samples is evidenced by the peak at 410-420 cm^{-1}, attributed to Si-O-Si bending vibrations. However, this peak was most prominent in the Si-TiO2 sample (414 cm^{-1}) and appeared to shift to higher wavenumbers (477 cm^{-1}) in the Si-ZnO. This shift may indicate different interactions between the silica nanoparticles and the metal dopants. The Si-TiO2 sample exhibited the most intense peaks, suggesting a higher degree of crystallinity or order in the membrane structure. The unique peak at 588 cm^{-1} can be attributed to Ti-O-Si vibrations, indicating the successful incorporation of Ti into the silica network. The enhanced intensity of the PSU peaks (e.g., 1151 cm^{-1} and 1584 cm^{-1}) suggests that Ti incorporation may lead to a more ordered polymer structure. The absence of the 580-590 cm^{-1} peak (PSU ring deformation) suggests that Zn incorporation may affect the ring structure of the polymer. A new peak at 477 cm^{-1} (compared to 414 cm^{-1} in Si-TiO2) indicates a different Si-O-Si network structure, possibly due to the incorporation of ZnO. The variations in the peak intensities and slight shifts in the peak positions across the samples suggest different degrees of interaction between the nanoparticles and PSU matrix. Si-TiO2 showed the

most substantial evidence of nanoparticle-polymer interactions, with enhanced PSU peak intensities. Si-ZnO shows more significant alterations to the PSU structure, possibly indicating stronger or more disruptive interactions.

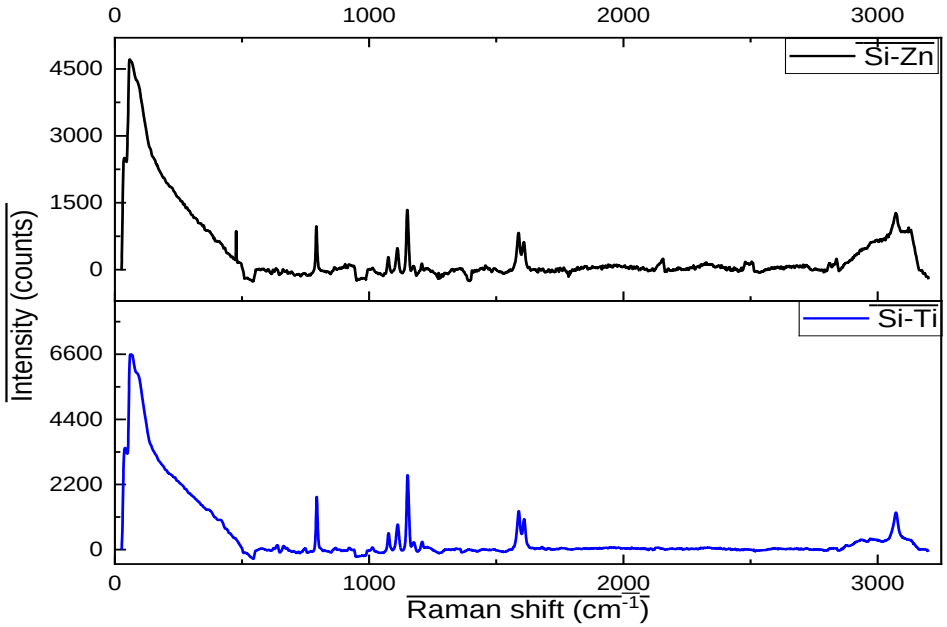

Figure 2 Raman patterns for both membranes: the pattern above is for **Si-**ZnO, and the one underneath is Si-TiO2.

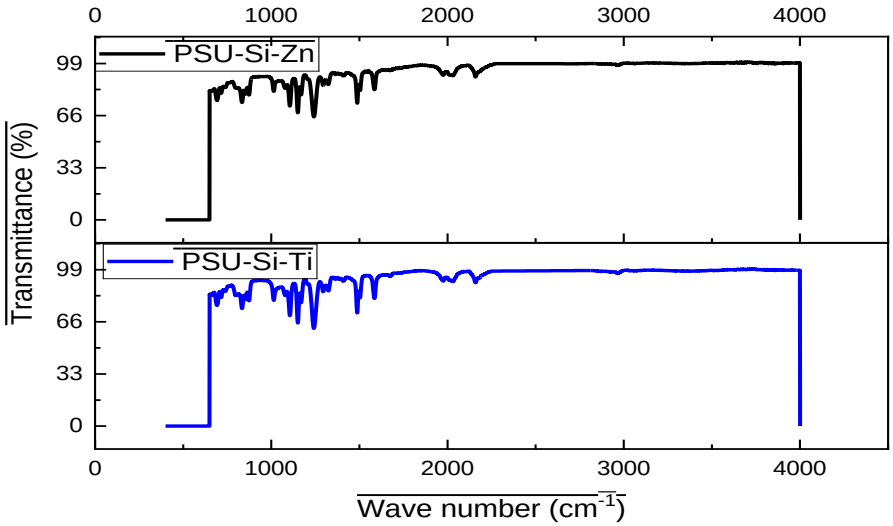

Figure 3 FT-IR patterns for both membranes: the pattern above is for **Si-ZnO**, and the one underneath is Si-TiO2 .

2.2. ***Surface area, pore characteristics and Dynamic Light Scattering (DLS)***

The surface area and pore characteristics of the nanocomposite membranes (Si-TiO2 and Si-ZnO) were analyzed using nitrogen adsorption-desorption isotherms. The key parameters derived from these measurements are listed in Table 1.

Table 1. **Surface area and pore characteristics of nanocomposite membranes**

Parameter	Si-TiO2	Si-ZnO
BET Surface Area (m^2/g)	0.03283	0.10564
Total Pore Volume (cm^3/g)	0.009074	0.001234
Average Pore Diameter (nm)	1105.4	8.644
BJH Pore Volume (cm^3/g)	-0.00019	9.735E-05
BJH Surface Area (m^2/g)	0.1655	0.07246
NLDFT Pore Volume (cm^3/g)	0.012695	0.001804
NLDFT Peak Pore Diameter (nm)	7.1022	9.631

The BET surface area of the Si-ZnO membrane showed (0.10564 m^2/g), and that of the Si-TiO2 membrane (0.03283 m^2/g). The significantly higher surface area suggests a greater number of available adsorption sites, which could enhance its interaction with water molecules and potentially improve its desalination performance [5,26]. The Si-ZnO membrane exhibited a considerably higher surface area than Si-TiO2. Interestingly, the Si-TiO2 membrane exhibited a higher total pore volume (0.009074 cm^3/g) than the Si-ZnO membrane (0.001234 cm^3/g). This suggests that the pore structure of the Si-TiO2 membrane might be composed of larger, more open pores, while the Si-ZnO membrane may have a much denser structure with limited pore space [5,27].

The average pore diameters calculated from the BET analysis showed significant membrane variations. The Si-TiO2 membrane exhibited an exceptionally large average pore diameter (1105.4 nm), consistent with its low surface area and relatively high pore volume, whereas the Si-ZnO membrane showed the smallest average pore diameter (8.644 nm), indicating a structure with predominantly small pores [27]. BJH analysis provides insights into the mesoporous structure of the membrane. This demonstrates that the Si-ZnO membrane has a very low BJH pore volume and surface area. The Si-TiO2 membrane showed a negative BJH pore volume, possibly due to limitations in the BJH model for materials with very large [28]. Nonlocal density functional theory (NLDFT) analysis provides a more accurate assessment of the pore size distribution, particularly for microporous and mesoporous materials. The NLDFT pore volumes are generally higher than those obtained from the BJH analysis, with the Si-TiO2 showing a value of (0.012695 cm^3/g) and the Si-ZnO membrane showing (0.001804 cm^3/g). The peak pore diameters from the NLDFT analysis show that the peak pore size of the Si-ZnO membrane was (9.631 nm), and that of the Si-TiO2 membrane (7.1022 nm).

Dynamic Light Scattering (DLS) analysis revealed distinct size distributions for each nanocomposite, indicating successful synthesis and size control. Table 2 and figure 3 summarize the key parameters for each sample.

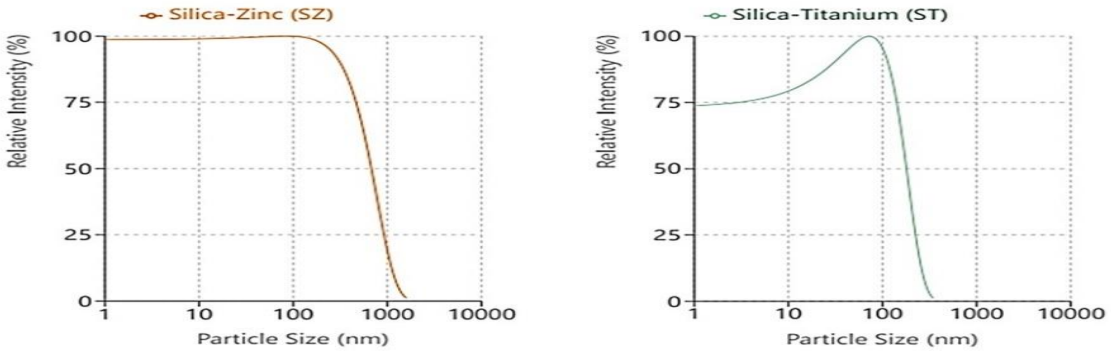

Figure 4 Particle size for both nanocomposites

Table 2. **DLS analysis results for nanocomposite samples**

Sample	Mean Diameter (nm)	Standard Deviation (nm)	Polydispersity Index (PDI)
ST	72.4	91.6	1.60
SZ	83.2	504.3	36.71

The incorporation of titanium led to a significant reduction in the particle size, with a mean diameter of 72.4 nm and a standard deviation of 91.6 nm. The lower PDI (1.60) indicates a more monodisperse distribution than that of pure silica nanoparticles [8,29]. This size reduction could be due to the titanium precursor acting as a nucleation site and promoting the formation of smaller, more uniform particles. The silica-zinc nanocomposite exhibited a mean diameter of 83.2 nm, with a standard deviation of 504.3 nm. The high PDI (36.71) indicates a polydisperse sample. The incorporation of zinc resulted in smaller particles than pure silica, possibly because zinc ions influenced the silica network formation and limited particle growth [8,29].

The zeta potential measurements for both nanocomposite samples in Table 3 reveal the critical characteristics of their surface properties and stability in aqueous environments. These properties have significant implications for the potential use of these membranes in water desalination. The silica-titanium nanocomposite exhibited a zeta potential of -34.4 mV with a deviation of 13.5 mV. This highly negative zeta potential indicates a strong negative surface charge, which is beneficial for colloidal stability [9,30].

Table 3. Illustrated zeta potential analysis for nanocomposite samples

Sample	Nanocomposite	Zeta Potential (mV)	Zeta Deviation (mV)	Conductivity (mS/cm)
1	**Silica-Ti**	**-34.4**	**13.5**	**0.052**
2	**Silica-Zn**	**-6.29**	**3.5**	**0.0547**

In terms of desalination membranes, this negative charge can repel negatively charged foulants, potentially reducing membrane fouling [10]. The high magnitude of the zeta potential (>30 mV in absolute value) suggests good stability in aqueous suspensions, which is crucial for maintaining consistent performance in desalination. A conductivity of 0.0520 mS/cm indicates a low ionic concentration in the suspension, which is favorable for maintaining the electrical double layer around the particles. In contrast, the silica-zinc nanocomposite showed a markedly different zeta potential of -6.29 mV with a deviation of 3.50 mV. This value is considerably closer to zero than that of the other sample, indicating a much weaker surface charge. In desalination applications, this near-neutral surface charge may increase particle aggregation and potentially increase fouling propensity. The low absolute zeta potential (<10 mV) suggests that this nanocomposite may have lower colloidal stability, which could affect its long-term performance and distribution within a polymer matrix for membrane fabrication. The conductivity (0.0547 mS/cm) was similar to that of the silica-titanium sample, suggesting comparable ionic environments. The zeta potential distribution graphs provided in Table 3 offer additional insights into the behavior of the nanocomposites. The silica-titanium nanocomposite exhibited broader peaks in its zeta potential distribution, as evidenced by its more significant zeta deviations. This broader distribution suggests a more heterogeneous surface charge, which could be beneficial for providing multiple interaction sites within the desalination membrane matrix. The silica-zinc nanocomposite displayed a narrower and more symmetrical peak, indicating a more uniform surface charge distribution. However, its proximity to zero potential raises concerns regarding stability in aqueous suspensions [9,30].

2.3. Scanning Electron Microscope, Energy-dispersive X-ray (SEM-EDX), and Transmission Electron Microscopy (TEM)

The SEM images of the synthesized nanocomposites are shown in Figure 5. This revealed distinct morphological features characteristic of silica-based nanoparticles modified with titanium and zinc. Incorporating titanium into the silica matrix resulted in a slightly rougher surface texture than that of pure silica nanoparticles [31,32].

A B

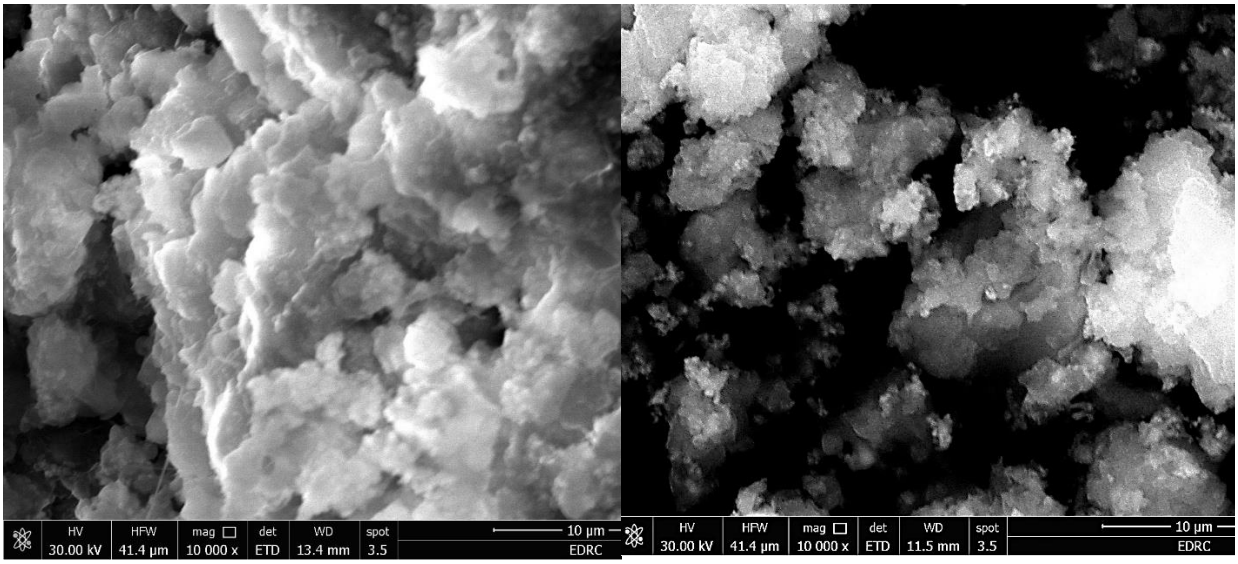

Figure 5 SEM images for both nanocomposites (A is Si-TiO2 and B is Si-ZnO)

The particles maintained a generally spherical shape with visible surface irregularities. This texture change suggests the successful doping of titanium into the silica structure, which could enhance the photocatalytic properties of the material and potentially improve its performance in water treatment applications [32]. The silica-zinc nanocomposite exhibited a more pronounced aggregation tendency than the silica-titanium samples [33]. This morphology indicates strong interactions between the silica matrix and zinc ions, which could enhance the antimicrobial properties of the final membranes.

The SEM images of the PSU-nanocomposite samples in Figure 6 demonstrate the integration of the synthesized nanocomposites into the polysulfone matrix, providing insights into the final membrane structure and its potential performance in desalination applications.

A B

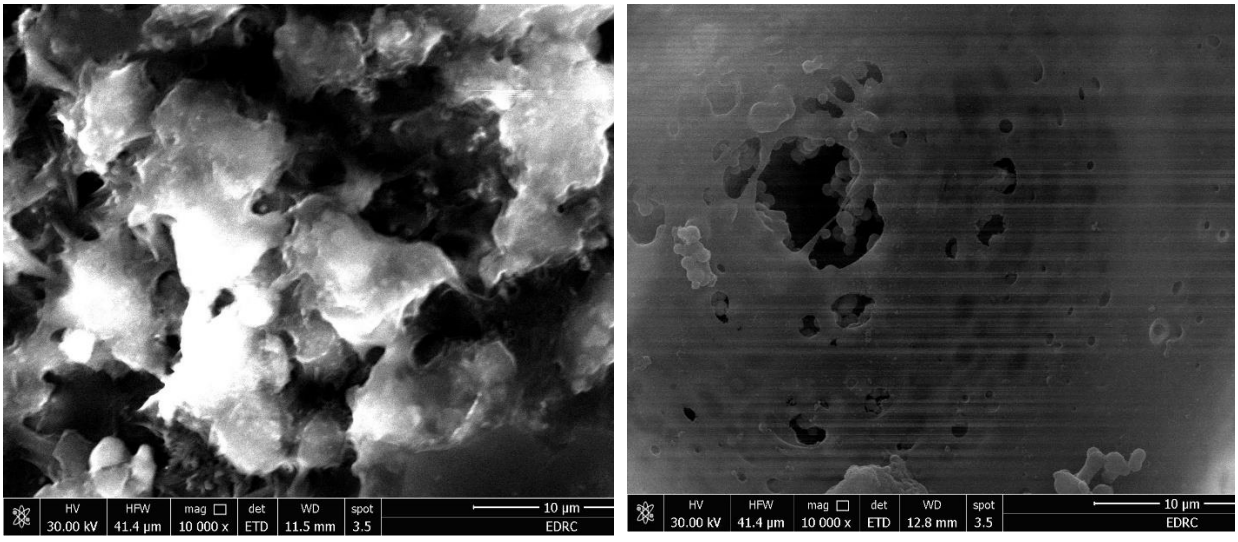

Figure 6 SEM images for both PSU-nanocomposites (A is PSU-Si-TiO2 and B is PSUSi-ZnO)

The image shows that incorporating the silica-titanium nanocomposite into PSU resulted in evenly distributed nanoparticles, with some areas showing slight aggregation.

This texture could increase the surface roughness, potentially enhancing the antifouling properties and water flux of the membrane. The PSU-Silica-Zinc composite exhibited a relatively uniform dispersion of nanoparticles with visible clusters. The surface appeared to have a fine granular texture, which may contribute to the increased surface area and potentially enhance the membrane's antimicrobial properties due to zinc, exhibiting a unique surface morphology with a fine and granular

texture. The pores appear as small structures that can improve salt rejection while maintaining a good water flux. Zinc is believed to impart antimicrobial properties, which may help reduce biofouling during desalination.

The SEM analysis of the nanocomposites and PSU-nanocomposite membranes indicated the successful synthesis and integration of silica-based nanoparticles modified with titanium and zinc into the polysulfone matrix. The EDX spectrum of the Si-TiO2 nanocomposite shows strong silicon (Si) and oxygen (O) peaks, confirming the successful synthesis of SiO2 nanoparticles (Figure 10A). Additionally, it shows clear titanium (Ti) peaks, confirming the successful incorporation of Ti into the silica matrix (Figure 6A). The relative intensities of the Si, O, and Ti peaks provide insight into the Ti doping level. The presence of Ti is crucial for the potential photocatalytic properties, which could enhance the antifouling capabilities of the final membrane. The C peak intensity may be slightly higher than that in pure silica owing to the Ti-organic complexes formed during synthesis. The data in Figure 7 reveal distinct zinc (Zn) peaks alongside Si and O, indicating the successful synthesis of the Silica-Zinc nanocomposite. The Si-ZnO ratio provides information on the degree of zinc incorporation. The presence of Zn is essential for imparting antimicrobial properties to the nanocomposite, which is beneficial for biofouling resistance in desalination membranes. Any observed shifts in the O peak position or intensity relative to pure silica might indicate the formation of Zn-O-Si bonds.

Incorporating Si-ZnO nanoparticles into polysulfone membranes provides a comprehensive strategy for reducing biofouling, organic fouling, and scaling, leading to enhanced filtration efficiency and durability. Zinc oxide exhibits antimicrobial properties, and its combination with silica produces a surface that is unfavorable for microbial growth, thereby reducing biofilm formation and minimizing biofouling [34].

A

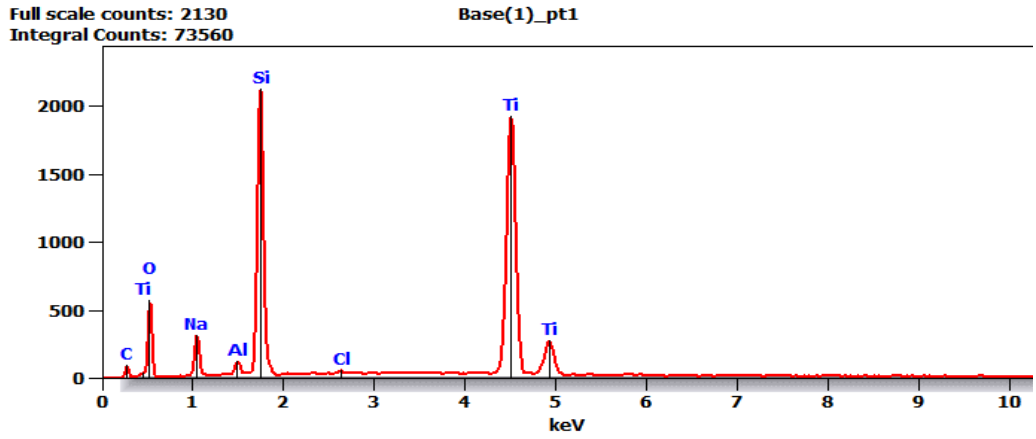

B

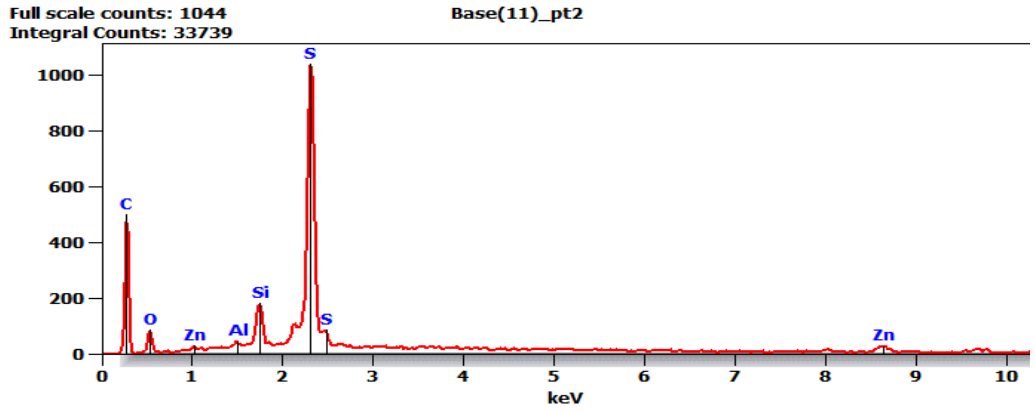

Figure 7 EDX for both samples (A is PSU-Si-TiO2 and B is PSU-Si-ZnO)

The EDX spectrum of the membranes (PSU-nanocomposites) in Figure 7 shows peaks characteristic of PSU (C, O, S) and silica (Si, O) (Figure 8). In addition to the peaks observed, clear Ti peaks are visible, confirming the presence of titanium in the nanocomposite. The relative intensities of Si, Ti, and PSU-related peaks provide information on the distribution of the nanocomposite within the polymer matrix. The presence of Ti may enhance the membrane's photocatalytic properties, potentially improving its anti-fouling performance in desalination applications. The spectrum also shows distinct Zn peaks alongside those of PSU and silica, indicating the successful incorporation of the Silica-Zinc nanocomposite into the PSU matrix. The Zn: Si and Zn: S ratios provide insights into the distribution of zinc within the nanocomposite and its

integration into the polymer structure. The presence of Zn is crucial for imparting antimicrobial properties to the membrane, which could significantly reduce biofouling in desalination processes.

The EDX analysis of the nanocomposites and PSU-nanocomposite membranes provides strong evidence for the successful synthesis and integration of silica-based nanoparticles modified with titanium and zinc into the polysulfone matrix. The presence of characteristic peaks for Si, Ti, and Zn in their respective nanocomposites validates the effectiveness of the green synthesis method using citrus peel extract. It confirms the successful synthesis of the nanocomposites and demonstrates the potential of eco-friendly approaches in creating advanced materials for desalination applications. The co-existence of peaks from PSU and nanocomposites in the PSU-nanocomposite samples confirms successful incorporation, which is crucial for enhancing membrane properties. Furthermore, nanocomposite-related peaks in membrane samples indicate that the nanoparticles are retained during the phase inversion. This retention is essential for imparting desired properties to the desalination membranes, ensuring that the benefits of the nanocomposites are maintained in the final product. The EDX results suggest several potential enhancements for desalination performance. The presence of Ti in the nanocomposites indicates possible photocatalytic properties, which could contribute significantly to fouling reduction in the membranes [35]. The detection of Zn implies possible antimicrobial properties, essential for protecting against biofouling, a significant challenge in desalination procedures [36]. Additionally, observed changes in O: C ratios in nanocomposite membranes compared to pure PSU may suggest altered surface hydrophilicity [11]. This could have important implications for water permeability and salt rejection, two key performance metrics for desalination membranes. The relative peak intensities in the EDX spectra provide valuable insights into nanoparticle loading and distribution within the membranes. It is crucial for optimizing membrane performance, as it allows for fine-tuning of the nanocomposite content to achieve the desired balance of properties. Together, the SEM analysis and the EDX results offer a comprehensive understanding of the composition and structure of the nanocomposite membrane that is critical for determining structure-property relationships and optimizing the membranes for desalination applications.

The significant aggregation of nanoparticles in PSU-Si-Zn membranes, as observed through SEM and DLS analyses, can indeed affect membrane performance in several ways. Aggregated particles create irregularities on the membrane surface, resulting in non-uniform hydrophilic and hydrophobic areas. This unevenness can negatively impact filtration efficiency and antifouling properties. Additionally, it can compromise the structural integrity of the membrane, potentially making it less durable under mechanical stress or prolonged operation. The particle clusters may block membrane pores or reduce their effective size, hindering fluid flow. Consequently, this results in lower permeability, compromising the overall functionality of the membrane. However, using the QCM, the results showed good salt rejection, which is attributed to sonicating the solution before placing it on the QCM disc, in addition to the antimicrobial results [37–39].

Transmission Electron Microscopy (TEM) was employed to analyze the nanostructure of nanocomposite polysulfone (PSU) membranes: Si-TiO2 and Si-ZnO. The TEM images in Figure 8 provide valuable insights into the size, shape, distribution, and aggregation of nanoparticles within the polymer matrix, which are crucial factors affecting membrane performance in desalination applications.

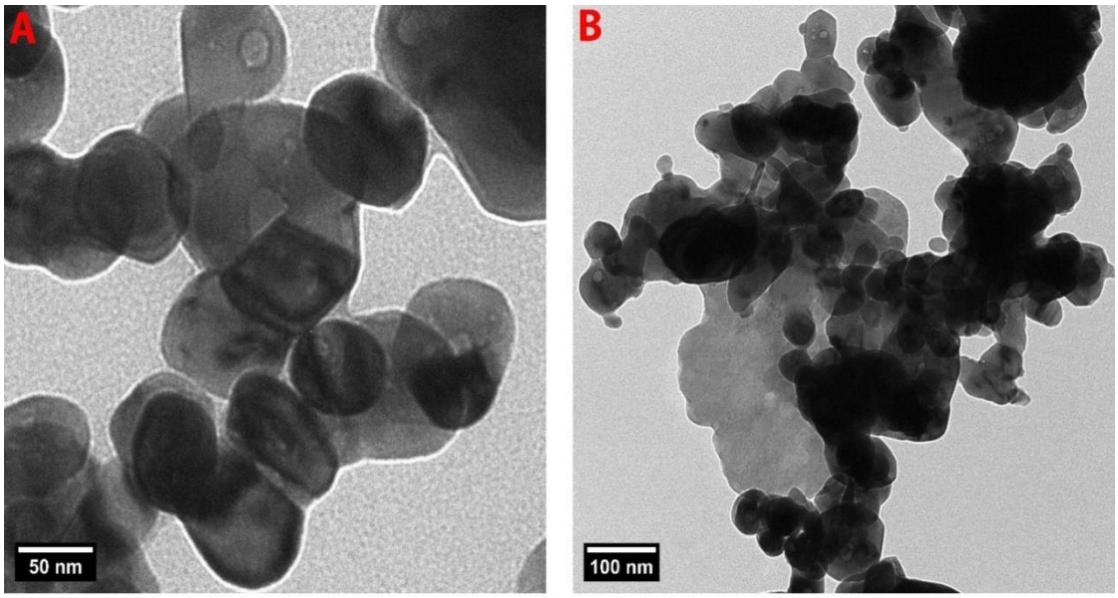

Figure 8 TEM images for both membranes where A is Si-TiO2 and B is Si-ZnO

A B

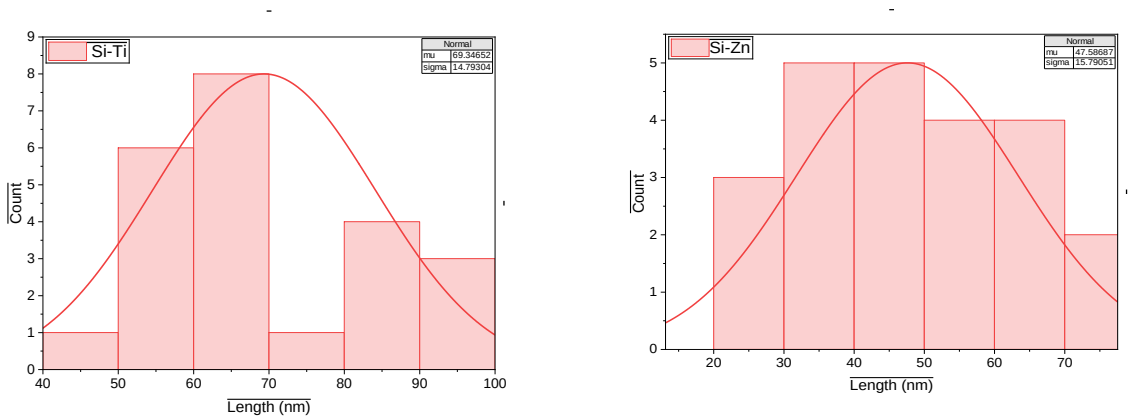

Figure 9 TEM histogram distribution plot for both membranes (A is Si-TiO2 and B is Si-ZnO)

The Si-TiO2 nanocomposite exhibits well-defined spherical nanoparticles with sizes ranging from 40 to 100 nm with an average diameter of 69.34 nm in Figures 8 and 9 [40]. The particles show a relatively uniform distribution throughout the imaged area with moderate aggregation. The clear boundaries between particles suggest good dispersion within the PSU matrix [41]. Due to the spaces between particle clusters, this structure may enhance the mechanical strength of the membrane while maintaining adequate permeability. The Si-ZnO sample displays irregularly shaped nanoparticles with sizes varying from 10 to 100 nm with an average of 47.58 nm illustrated in Figure 9. The particles show a high degree of aggregation, forming fused clusters. This non-uniform distribution and fusion of particles may create larger pores in some areas of the membrane, potentially affecting its selectivity. The irregular shapes could result from the interaction between ZnO and Si during nanoparticle formation or from the fusion of smaller particles [41].

2.4. Quartz Crystal Microbalance Analysis

The Quartz Crystal Microbalance (QCM) analysis was utilized to evaluate the desalination performance of both polysulfone (PSU) nanocomposite membranes. This technique offers valuable insights into the interactions between the membrane and salt by measuring frequency changes (ΔF) of a quartz crystal coated with the membrane material when exposed to KCl and MgCl salt solutions. In QCM analysis, a decrease in frequency (negative ΔF) indicates mass adsorption onto the membrane surface, whereas an increase (positive ΔF) suggests mass desorption or rejection. A smaller negative ΔF or a positive ΔF signifies better salt rejection for desalination membranes, indicating less salt adsorption or effective salt repulsion.

Salt adsorption can sometimes indicate that the membrane material interacts preferentially with certain ions. This might enhance selectivity by blocking specific salts more effectively, potentially contributing to improved salt rejection. However, this effect depends on the molecular interactions and the design of the membrane's active layer [42].

2.4.1. Impact of KCL on the whole process.

A 5 MHz AT-cut quartz crystal was used for the QCM measurements, and the membranes were subjected to a 0.5 M KCl solution. Frequency changes were recorded over 30 minutes to assess immediate and prolonged membrane-salt interactions [43,44].

Table 4: Quantitative results of QCM

Features Membrane		**PSU-Silica-Titanium**	**PSU-Silica-Zinc**
QCM using KCL solution	Initial ΔF (0-5 min) (Hz)	-42	-61
	Final ΔF (30 min) (Hz)	-58	-89
	Rate of frequency change (Hz/min)	-0.53	-0.93

Salt adsorption per unit area (µg/cm^2)	1.02	1.57
Initial rate of frequency change (first 30 seconds of exposure) Hz/s	-38	-45
Rate of frequency change over the 30 minutes (Hz/min)	-0.53	-0.93

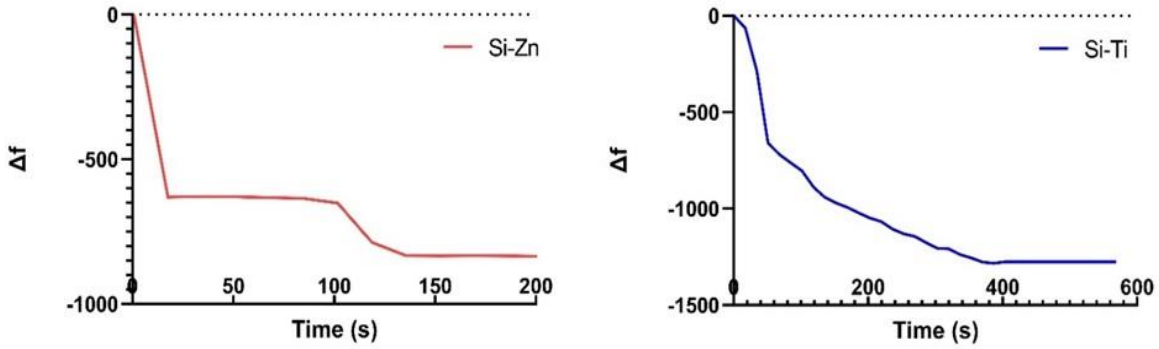

Figure 10 senso-gram curve of both membranes against KCl solution.

The PSU-Silica-Titanium membrane in figure 10 and table 4 demonstrated markedly improved salt rejection with an initial ΔF of -42 Hz and a slower rate of change (-0.53 Hz/min). This enhancement can be attributed to the Ti-O-Si bonds altering surface charge and pore structure, creating a more effective barrier against salt ions. The PSU-Silica-Zinc membrane improved over the PSU-Si-TiO2 membrane, with an initial ΔF of -61 Hz. However, its rate of frequency change (-0.93 Hz/min) was the highest among the samples, suggesting potential long-term stability issues or ongoing salt accumulation. To correlate QCM data with real-world desalination performance, we can use the Sauerbrey equation, which relates frequency change to mass adsorption:

$$\Delta F = -Cf \times \Delta m \quad (1)$$

Where Cf is the sensitivity factor of the crystal (56.6 Hz·µg^-1·cm^2 for a 5 MHz crystal) and Δm is the mass change per unit area. Each membrane's salt adsorption per unit area can be estimated using this equation.

These values provide a quantitative measure of salt rejection efficiency. Lower adsorption values indicate better salt rejection, suggesting superior desalination performance. While QCM primarily measures mass changes, it can also provide insights into water flux. The initial rate of frequency change (first 30 seconds of exposure) can indicate water uptake. These values suggest that the PSU-Si-ZnO membrane has a higher water uptake, likely due to its hydrophilic nature. However, this also correlates with its poor salt rejection. The rate of frequency change over the 30 minutes provides insights into long-term stability and fouling resistance:

The PSU-Silica-Titanium membrane shows promising stability, while the PSU-Silica-Zinc membrane's high rate of change indicates potential long-term performance issues. Based on the QCM analysis, we can rank the membranes for desalination performance. The PSU-Si-TiO2 has a respectable balance of salt rejection (1.02 µg/cm^2 adsorption) and stability (-0.53 Hz/min change rate), and PSU-Si-ZnO has moderate improvement over PSU-Si-TiO2 but potential long-term issues, QCM analysis of polysulfone (PSU) nanocomposite membranes against KCl solutions provides crucial insights into their potential performance as desalination membranes [45].

The QCM data revealed varying salt rejection efficiency among both nanocomposite membranes.
PSU-Si-TiO2 and PSU-Si-ZnO membranes show promising antifouling properties and durability, making them competitive alternatives for specific applications. Commercial membranes excel in salt rejection and scalability but may face challenges with fouling [46].

The PSU-Si-TiO2 membrane demonstrated the second-highest salt rejection efficiency [47]. Incorporating titanium into the silica nanoparticles creates a more tortuous path for salt ions, increasing the membrane's selectivity. This enhanced performance may be due to the formation of Ti-O-Si bonds, which alter the membrane's surface charge and pore structure, improving salt rejection capabilities. Interestingly, the PSU-Si-ZnO membrane showed moderate salt rejection, performing better than the pure PSU-Si membrane but not reaching the levels of the titanium-doped sample. The presence of zinc ions in the nanocomposite structure likely contributes to a more negatively charged membrane surface, which could repel chloride

ions to some extent. However, the larger ionic radius of zinc compared to titanium might result in less efficient pore size control, explaining its intermediate performance. Additionally, QCM analysis provided insights into the membrane's water flux characteristics. The frequency shifts observed during the initial exposure to the KCl solution correlate with the membranes' water permeability. The PSU-Si-TiO2 sample showed a good balance between salt rejection and water flux.

The titanium doping optimizes the pore structure and surface properties, allowing for efficient water transport while maintaining high salt rejection. This balance is crucial for desalination applications in practice, where high salt rejection and adequate water flux are necessary for efficient operation. The PSU-Si-TiO2 membrane also showed good stability, with minimal frequency drift over extended exposure periods. This stability can be linked to the photocatalytic properties of titanium dioxide, which may help in the degradation of organic foulants, thereby maintaining membrane performance over time. The PSU-Si-TiO2 membrane presents an attractive balance between salt rejection, water flux, and stability, making it a strong contender for practical desalination applications. Its performance characteristics suggest it could be particularly suitable for brackish water desalination, where moderate salt concentrations are encountered [45,48].

2.4.2. Impact of MgCl Solution on the whole process

The PSU-Si-ZnO membrane in figure 11 and table 4 initially showed no change in frequency but experienced a rapid decline starting at 55 seconds, ultimately reaching a final frequency shift (Δf) of -260 Hz. This behavior indicates swift and significant adsorption of MgCl, with the membrane stabilizing around 80 seconds.

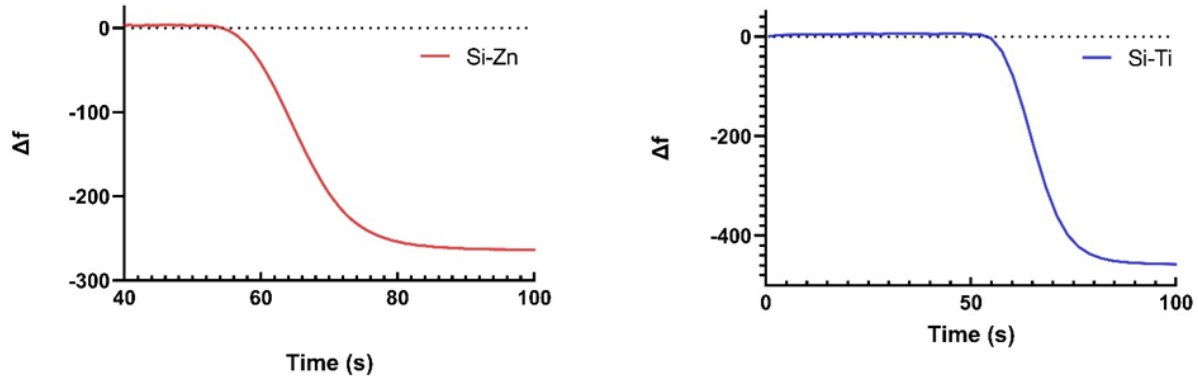

Figure 11 senso-gram curve of both membranes against MgCl solution explains the desalination ability of the membranes.

The absence of an initial positive Δf suggests limited interaction with water. While the high adsorption capacity could be advantageous for selective ion removal, it may not be ideal for general desalination due to the potential for rapid saturation. In contrast, the PSU-Si-TiO2 membrane displayed the most significant frequency decrease among all the samples, achieving a final Δf of -470 Hz. Like the Si-ZnO membrane, it showed no initial change but experienced a steep drop after 50 seconds and stabilized around 75 seconds. This behavior indicates that the Si-TiO2 membrane has the highest adsorption capacity for MgCl of all the tested membranes. The rapid and extensive adsorption suggests that the Si-TiO2 membrane could be highly effective in removing specific ions but might require more frequent regeneration in continuous desalination applications.

Compared to the membranes' performance, we can rank their salt rejection efficiency based on the final Δf values: Si-ZnO> Si-TiO2. However, it's crucial to know that smaller negative Δf values, which frequently signify increased salt rejection, can also indicate a lower degree of overall interaction with the salt solution. Regarding adsorption capacity, the ranking is reversed: Si-TiO2> Si-ZnO. The high adsorption capacity in the metal-doped membranes could be beneficial for removing specific ions, but it may not be ideal for general desalination. The QCM analysis reveals distinct behaviors for each nanoparticle-decorated membrane when exposed to MgCl salt. The Si-ZnO and Si-TiO2 membranes exhibit high salt adsorption capacities, which could be advantageous for specific ion removal applications but may require optimization for general desalination use the results of the QCM are summarized in table 5. The steepness of the Δf decrease indicates that the adsorption kinetics for the Si-TiO2 and Si-ZnO membranes are comparable. The rapid adsorption rates of these membranes suggest efficient ion capture, which may be beneficial in specific water treatment applications; however, it could also lead to quicker saturation and a more frequent need for regeneration in continuous desalination processes [44,45,49].
Both nanoparticles are synthesized in situ, with silica nanoparticles having a strong bind between silica and metal oxides (nanocomposites), in addition to the strong bonds between Polysulfone and Silica metal oxides making it hard to leach out [7,50].

2.5. Antimicrobial Activity

The antimicrobial activity tests were conducted to assess the effectiveness of the membranes with Inhibition zone that shows how effective the membrane is against different strains of bacteria, the Minimum Inhibitory Concentration (MIC) is defined as the lowest concentration of an antimicrobial agent that prevents visible growth of a microorganism, while the Minimum Bactericidal Concentration (MBC) is the lowest concentration needed to kill 99.9% of the bacterial population. The results in fig 8 showed that the membranes exhibited significant activity against the tested organisms. However, it was noted that the PUS-Si-ZnO membrane had low MIC and MBC values against E. coli. The proximity of the MIC and MBC values indicates that the agent has both bacteriostatic and bactericidal properties, making it a promising candidate for antimicrobial applications. Overall, the membranes demonstrated antimicrobial activity, suggesting they possess anti biofouling properties [36,40].

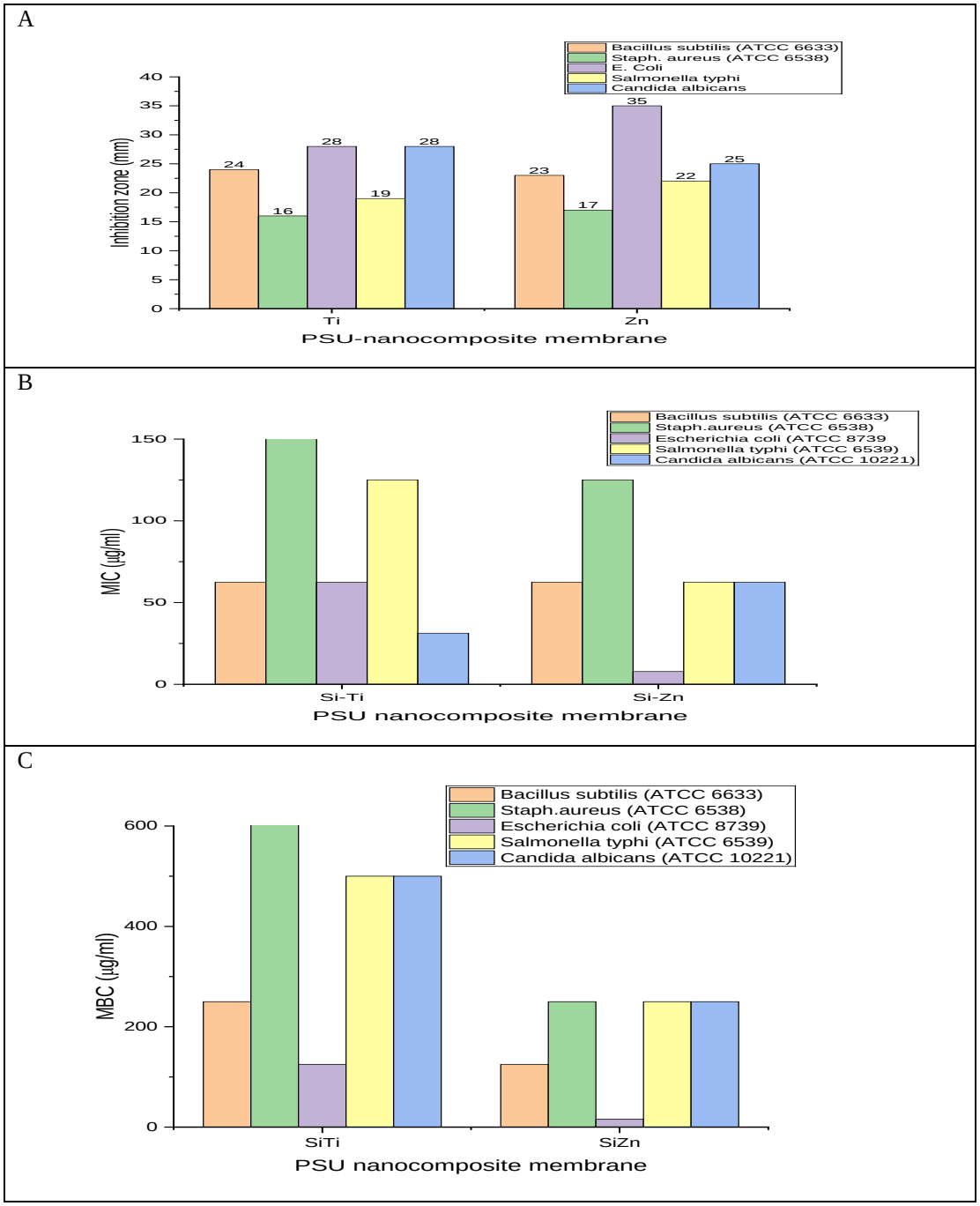

Figure 12 Antimicrobial activity for both samples against 5 strains

3. Materials and Methods

3.1. Chemical and reagents

Zinc acetate (≥98% purity, analytical grade), titanium tetrachloride (99.9% purity, reagent grade), sodium silicate (97% purity, technical grade), and dimethylformamide (DMF) purity of ≥99.8% (anhydrous) were acquired from El Gomhoureya for Drugs Trade and Medical Supplies, Cairo, Egypt. Polysulfone was acquired from Solvay Advanced Polymers GmbH, Germany, and fresh citrus (orange and lemon) peels were purchased from a local market in Egypt for the green synthesis.

3.2. Green synthesis of nanoparticles

The citrus peels were thoroughly cleaned to remove any potential contaminants. First, the peels were washed with tap water, manually brushed to remove surface impurities, and rinsed with distilled water to remove any residual contaminants. After air-drying at room temperature, 20 g of the cleaned peels were immersed in 500 ml of distilled water in a borosilicate glass beaker. The mixture was then heated on a calibrated hot plate at a constant temperature of 50°C (±1°C) for 2 h to facilitate the extraction of bioactive compounds. The solution was then allowed to cool to room temperature and filtered through Whatman No. 1 filter paper to remove solid residues. The resulting extract was stored at 4°C in amber glass bottles to prevent the photodegradation of light-sensitive compounds.

3.3. Preparation of nanocomposites

A modified in situ approach was used to prepare metal-doped silica nanocomposites. This involved adding 0.4 g of the respective metal precursor (20% w/w relative to the silica content) to the sodium silicate solution before introducing the citrus peel extract. Two grams of sodium silicate and 0.4 g of titanium tetrachloride were co-dissolved in 250 mL of distilled water at 55°C (±1°C) to prepare the silica-titanium nanocomposite. After cooling, 100 mL of citrus peel extract was added dropwise. The reaction was maintained at room temperature for 2-3 hours under constant stirring at 400 rpm. The solution was then left overnight in a dark and clean environment. Subsequently, the solution was placed in a centrifuge and spun at 8000 rpm for 5 min. The samples were washed with distilled water and centrifuged again to remove any unwanted residues. Finally, the solution was transferred to a plate and allowed to dry. The procedure for preparing the Silica-Zinc Nanocomposite was similar to that of the Silica-Titanium Nanocomposite, with the only difference being the substitution of 0.4 g of zinc acetate for titanium tetrachloride.

*3.4. Polymer preparation and membrane fabrication***

The polysulfone (PSU) solution was prepared under controlled conditions to ensure consistency. In a clean, dry borosilicate glass beaker, 2.5 g of PSU beads were added to 100 mL of anhydrous N, N-dimethylformamide (DMF). The mixture was heated to 50°C (±1°C) on a hotplate magnetic stirrer and stirred at 300 rpm for 3 h until complete dissolution, resulting in a clear, homogeneous solution. The fabrication of nanocomposite membranes followed a standardized procedure, with minor adjustments depending on the specific nanocomposite incorporated. In each case, 2 mg of the respective nanoparticle solution (representing 2% w/w of the total solution) was placed in a clean beaker and heated to 50°C (±1°C) on a hotplate magnetic stirrer. Subsequently, 98 mL of the prepared PSU solution was added dropwise at a rate of approximately 1 mL/min under constant stirring at 200 rpm.

The solution was maintained at 50°C for an additional 4-5 hours to ensure thorough mixing and enable potential chemical interactions between the nanoparticles and the polymer matrix. After the mixing period, the solutions were allowed to cool to room temperature to prevent the formation of air bubbles. Membrane casting was performed using a microscope slide technique. A single drop of the cooled nanocomposite-polymer solution was carefully placed on a clean, level glass microscope slide. The slides were left undisturbed in a dust-free environment at room temperature (23 ±2°C) for 24 h to allow complete solvent evaporation and film formation. This process was repeated for each type of nanocomposite (PSU-Silica-Titanium and PSU-Silica-Zinc), ensuring that all parameters remained constant across the preparations to facilitate accurate comparisons of the resulting membranes.

4. Conclusion

In conclusion, water desalination is a crucial method for providing potable water. Although polysulfone (PSU) membranes have advantages, they also have drawbacks, including biofouling and restricted salt rejection. This research focused on developing a PSU membrane enhanced with silica-titanium (Si-TiO2) and silica-zinc (Si-ZnO) nanocomposites. Both Si-ZnO and Si-TiO2 membranes exhibited high salt adsorption capacities, suggesting advantages for specific ion

removal, although optimization is needed for general desalination. The rapid adsorption rates indicate efficient ion capture but may lead to quicker saturation in continuous desalination processes.

4. Conflicts of Interest: The authors declare no conflicts of interest

5. Acknowledgments:

I would like to express my deepest gratitude to Mr. Sameh H. Ismail, a researcher in the Faculty of Nanotechnology for postgraduate studies, for his invaluable guidance, constant encouragement, and insightful feedback throughout the development of this research. His expertise and unwavering support have been instrumental in shaping the direction of this work. Without his help, this project would not have reached its full potential. I am truly grateful for his time and effort in this project, and I look forward to future collaborations.

6. Author Contributions: All authors contributed equally to this work

7. References

[1] H. Maleki, P. Asadi, A. Moghanian, S. Safaee, I.M.R. Najjar, A. Fathy, Hybrid PLA-based biocomposites produced by DLP 3D printer with alumina and silica nanoparticles, Mater. Today Commun. 42 (2025) 111469. https://doi.org/https://doi.org/10.1016/j.mtcomm.2024.111469.

[2] A. Seif, A. Fathy, M.M. Awd Allah, S.F. Mahmoud, D.I. Saleh, A.A. Megahed, To what extent can the drilling process affect the drilling performance in A l-mesh/GFRE hybrid composites?, Polym. Compos. (n.d.).

[3] E. Eren, A. Sarihan, B. Eren, H. Gumus, F.O. Kocak, Preparation, characterization and performance enhancement of polysulfone ultrafiltration membrane using PBI as hydrophilic modifier, J. Memb. Sci. 475 (2015) 1–8.

[4] J. Zhang, Z. Wang, X. Zhang, X. Zheng, Z. Wu, Enhanced antifouling behaviours of polyvinylidene fluoride membrane modified through blending with nano-TiO2/polyethylene glycol mixture, Appl. Surf. Sci. 345 (2015) 418–427.

[5] L. Pellenz, C.R.S. de Oliveira, A.H. da Silva Júnior, L.J.S. da Silva, L. da Silva, A.A.U. de Souza, S.M. de A.G. Ulson, F.H. Borba, A. da Silva, A comprehensive guide for characterization of adsorbent materials, Sep. Purif. Technol. 305 (2023) 122435.

[6] H. Ahmadian, T. Zhou, A.M. Sadoun, A.S. Kumar, A. Fathy, Q. Yu, G. Weijia, A. Wagih, Optimized ball milling and sequential addition of SiC and MWCNTs reinforcements for enhanced performance of copper hybrid composites, Results Eng. 24 (2024) 103471. https://doi.org/https://doi.org/10.1016/j.rineng.2024.103471.

[7] A.L. Mohamed, A.G. Hassabo, Modified Cellulose Acetate Membrane for Industrial Water Purification, Egypt. J. Chem. 65 (2022) 53–70.

[8] M. Balestrat, A. Lale, A.V.A. Bezerra, V. Proust, E.W. Awin, R.A.F. Machado, P. Carles, R. Kumar, C. Gervais, S. Bernard, In-situ synthesis and characterization of nanocomposites in the Si-Ti-N and Si-Ti-C systems, Molecules 25 (2020) 5236.

[9] A. Serrano-Lotina, R. Portela, P. Baeza, V. Alcolea-Rodríguez, M. Villarroel, P. Ávila, Zeta potential as a tool for functional materials development, Catal. Today 423 (2023) 113862.

[10] A. Lee, J.W. Elam, S.B. Darling, Membrane materials for water purification: design, development, and application, Environ. Sci. Water Res. Technol. 2 (2016) 17–42.

[11] S.C. Mamah, P.S. Goh, A.F. Ismail, N.D. Suzaimi, L.T. Yogarathinam, Y.O. Raji, T.H. El-badawy, Recent development in modification of polysulfone membrane for water treatment application, J. Water Process Eng. 40 (2021) 101835.

[12] R. Sirohi, Y. Kumar, A. Madhavan, N.A. Sagar, R. Sindhu, B. Bharathiraja, H.O. Pandey, A. Tarafdar, Engineered nanomaterials for water desalination: Trends and challenges, Environ. Technol. Innov. 30 (2023) 103108.

[13] H. Ahmadian, T. Zhou, M. Abd Elaziz, M. Azmi Al-Betar, A.M. Sadoun, I.M.R. Najjar, A.W. Abdallah, A. Fathy, Q. Yu, Predicting crystallite size of Mg-Ti-SiC nanocomposites using an adaptive neuro-fuzzy inference system model modified by termite life cycle optimizer, Alexandria Eng. J. 84 (2023) 285–300. https://doi.org/https://doi.org/10.1016/j.aej.2023.11.009.

[14] A. Iqbal, E. Cevik, A. Mustafa, T.F. Qahtan, M. Zeeshan, A. Bozkurt, Emerging developments in polymeric nanocomposite membrane-based filtration for water purification: A concise overview of toxic metal removal, Chem. Eng. J. (2024) 148760.

[15] N. Radulica, J.L. Sanz, A. Lozano, Dentin Bond Strength of Calcium Silicate-Based Materials: A Systematic Review of In Vitro Studies, Appl. Sci. 14 (2023) 104.

[16] I. Salahshoori, D. Nasirian, N. Rashidi, M.K. Hossain, A. Hatami, M. Hassanzadeganroudsari, The effect of silica nanoparticles on polysulfone–polyethylene glycol (PSF/PEG) composite membrane on gas separation and rheological properties of nanocomposites, Polym. Bull. 78 (2021) 3227–3258.

[17] M. Nur-E-Alam, S.A. Deowan, E. Hossain, K.S. Hossain, M.Y. Miah, M. Nurnabi, Fabrication of Polysulfone-Based Microfiltration Membranes and Their Performance Analysis, Water, Air, Soil Pollut. 235 (2024) 75.

[18] P. Kallem, I. Othman, M. Ouda, S.W. Hasan, I. AlNashef, F. Banat, Polyethersulfone hybrid ultrafiltration membranes fabricated with polydopamine modified ZnFe2O4 nanocomposites: Applications in humic acid removal and oil/water emulsion separation, Process Saf. Environ. Prot. 148 (2021) 813–824.

[19] S.S. Alterary, A.A. Alshahrani, F.M. Barakat, M.F. El-Tohamy, Selective-layer polysulfone membranes based on unfunctionalized and functionalized MoS2/polyamide nanocomposite for water desalination, Environ. Sci. Pollut. Res. (2024) 1–15.

[20] O.M.A. Shahlol, H. Isawi, M.G. El-Malky, A.E.-H.M. Al-Aassar, Performance evaluation of the different nano-enhanced polysulfone membranes via membrane distillation for produced water desalination in Sert Basin-Libya, Arab. J. Chem. 13 (2020) 5118–5136.

[21] H. Ghasemi, N. Abu-Zahra, N. Baig, I. Abdulazeez, I.H. Aljundi, Enhancing fouling resistance and separation performance of polyethersulfone membrane through surface grafting with copolymerized thermo-responsive polymer and copper oxide nanoparticles, Chem. Eng. J. Adv. 16 (2023) 100528.

[22] A. Fujishima, X. Zhang, D.A. Tryk, TiO2 photocatalysis and related surface phenomena, Surf. Sci. Rep. 63 (2008) 515–582.

[23] K. Bhattacharyya, B. Modak, C. Nayak, R.G. Nair, D. Bhattacharyya, S.N. Jha, A.K. Tripathi, The formation and effect of O-vacancies in doped TiO 2, New J. Chem. 44 (2020) 8559–8571.

[24] D. Gallach, A. Muñoz-Noval, V. Torres-Costa, M. Manso-Silván, Luminescence and fine structure correlation in ZnO permeated porous silicon nanocomposites, Phys. Chem. Chem. Phys. 17 (2015) 20597–20604.

[25] Ü. Özgür, Y.I. Alivov, C. Liu, A. Teke, M.A. Reshchikov, S. Doğan, V. Avrutin, S.-J. Cho, and H. Morkoç, A comprehensive review of ZnO materials and devices, J. Appl. Phys. 98 (2005).

[26] I. Ali, M. Suhail, Z.A. Alothman, A. Alwarthan, Recent advances in syntheses, properties and applications of TiO 2 nanostructures, RSC Adv. 8 (2018) 30125–30147.

[27] A.M. Elshahawy, S.M. Elkatlawy, M.S. Shalaby, C. Guan, J. Wang, Surface-engineered TiO2 for high-performance flexible supercapacitor applications, J. Electron. Mater. 52 (2023) 1347–1356.

[28] T. Kambe, T. Tsuji, K. Fukue, Zinc transport proteins and zinc signaling, Zinc Signals Cell. Funct. Disord. (2014) 27–53.

[29] Sangeeta, Onisha, N. Sandhu, C. Kumar, F. Mohajer, R. Tomar, Critical Review on Titania-Based Nanoparticles: Synthesis, Characterization, and Application as a Photocatalyst, Chem. Africa 7 (2024) 1749–1768.

[30] K. Dudek, M. Dulski, J. Podwórny, M. Kujawa, A. Gerle, P. Rawicka, Synthesis and Characterization of Silica-Titanium Oxide Nano-Coating on NiTi Alloy, Coatings 14 (2024) 391.

[31] J. Zhang, H. Liu, J. Wang, J. Shang, M. Xu, X. Zhu, C. Xu, H. Bai, X. Zhao, Bioinspired Hollow Mesoporous Silica Nanoparticles Coating on Titanium Alloy with Hierarchical Structure for Modulating Cellular Functions, J. Bionic Eng. 21 (2024) 1427–1441.

[32] E. Parra-Ortiz, L. Caselli, M. Agnoletti, M.W.A. Skoda, X. Li, D. Zhao, M. Malmsten, Mesoporous silica as a matrix for photocatalytic titanium dioxide nanoparticles: Lipid membrane interactions, Nanoscale 14 (2022) 12297–12312.

[33] S. Kumar, R. Seth, S. Panwar, K.K. Goyal, V. Kumar, R.K. Choubey, Morphological and optical studies of ZnO-silica nanocomposite thin films synthesized by time dependent CBD, J. Electron. Mater. 50 (2021) 3462–3470.

[34] A.S. Lashkenari, M.T.H. Mosavian, M. Peyravi, M. Jahanshahi, Biofouling mitigation of bilayer polysulfone membrane assisted by zinc oxide-polyrhodanine couple nanoparticle, Prog. Org. Coatings 129 (2019) 147–158.

[35] Y. Cui, L. Yang, Y. Yan, Z. Wang, J. Zheng, B. Li, Y. Feng, C. Li, M. Meng, Nature-mimicking fabrication of antifouling photocatalytic membrane based on Ti/BiOI and polydopamine for synergistically enhanced photocatalytic degradation of tetracycline, Korean J. Chem. Eng. 38 (2021) 442–453.

[36] S.-E. Jin, H.-E. Jin, Antimicrobial activity of zinc oxide nano/microparticles and their combinations against

pathogenic microorganisms for biomedical applications: From physicochemical characteristics to pharmacological aspects, Nanomaterials 11 (2021) 263.

[37] A. Sotto, A. Boromand, R. Zhang, P. Luis, J.M. Arsuaga, J. Kim, B. Van der Bruggen, Effect of nanoparticle aggregation at low concentrations of TiO2 on the hydrophilicity, morphology, and fouling resistance of PES–TiO2 membranes, J. Colloid Interface Sci. 363 (2011) 540–550.

[38] H.M. Ahmed, N.Y. Mohamed, M.A. El-Khateeb, M.M. Hefny, F.M. Abdel-Haleem, N. Ahmed, Synthesis, and characterization of magnetic nano-particles using opuntia extract, and its applications in wastewater treatment, Egypt. J. Chem. 67 (2024) 171–178.

[39] M.M. Salama, A.M. Abdo, A.A. Mousa, A.A. Shaheen, A.M. Elsayed, A.M. Soliman, Morus Alba Leaf Extract-Based Biogenic Production of Silver Nanoparticles: Characterization, Antibacterial, and Antiviral Evaluation, Egypt. J. Chem. 65 (2022) 605–615.

[40] M.G. Correa, F.B. Martínez, C.P. Vidal, C. Streitt, J. Escrig, C.L. de Dicastillo, Antimicrobial metal-based nanoparticles: A review on their synthesis, types and antimicrobial action, Beilstein J. Nanotechnol. 11 (2020) 1450–1469.

[41] L.F. Villalobos, Y. Xie, S.P. Nunes, K. Peinemann, Polymer and membrane design for low temperature catalytic reactions, Macromol. Rapid Commun. 37 (2016) 700–704.

[42] M.A. Ahmed, S.A. Mahmoud, A.A. Mohamed, Nanomaterials-modified reverse osmosis membranes: a comprehensive review, RSC Adv. 14 (2024) 18879–18906.

[43] W. Al-Gethami, D. Alhashmialameer, N. Al-Qasmi, S.H. Ismail, A.H. Sadek, Design of a novel nanosensors based on green synthesized CoFe2O4/Ca-alginate nanocomposite-coated QCM for rapid detection of Pb (II) ions, Nanomaterials 12 (2022) 3620.

[44] H.A. Huellemeier, N.M. Eren, J. Ortega-Anaya, R. Jimenez-Flores, D.R. Heldman, Application of quartz crystal microbalance with dissipation (QCM-D) to study low-temperature adsorption and fouling of milk fractions on stainless steel, Chem. Eng. Sci. 247 (2022) 117004.

[45] L. Wang, J. Song, C. Yu, The utilization and advancement of quartz crystal Microbalance (QCM): A mini review, Microchem. J. (2024) 109967.

[46] A.A. Alotaibi, A.K. Shukla, M.H. Mrad, A.M. Alswieleh, K.M. Alotaibi, Fabrication of polysulfone-surface functionalized mesoporous silica nanocomposite membranes for removal of heavy metal ions from wastewater, Membranes (Basel). 11 (2021) 935.

[47] J. Kamp, S. Emonds, M. Seidenfaden, P. Papenheim, M. Kryschewski, J. Rubner, M. Wessling, Tuning the excess charge and inverting the salt rejection hierarchy of polyelectrolyte multilayer membranes, J. Memb. Sci. 639 (2021) 119636.

[48] Y. Wen, X. Zhang, M. Chen, Z. Wu, Z. Wang, Characterization of antibiofouling behaviors of PVDF membrane modified by quaternary ammonium compound–combined use of QCM-D, FCM, and CLSM, J. Water Reuse Desalin. 9 (2019) 18–30.

[49] S.S. Ali, G.K. Hassan, S.H. Ismail, A.A. Ebnalwaled, G.G. Mohamed, M. Hafez, Exploration of PVC@ SiO2 nanostructure for adsorption of methylene blue via using quartz crystal microbalance technology, Sci. Rep. 13 (2023) 19621.

[50] S. Kandula, P. Jeevanandam, Synthesis of Silica@ Ni-Co mixed metal oxide core–shell nanorattles and their potential use as effective adsorbents for waste water treatment, Eur. J. Inorg. Chem. 2015 (2015) 4260–4274.

[48] EL-MESALLAMY, A., Alahwany, A., El-Zaidy, M., & Hussein, S. (2024). Eco-friendly Synthesis Of Zinc Oxide Nanoparticles by Garcinia cambogia and Evaluation of Their Obesity and Antimicrobial Activities. Egyptian Journal of Chemistry, 67(2), 17-27. doi: 10.21608/ejchem.2023.212794.8008

[49] Ahmed, H., Mohamed, N., El-Khateeb, M., Hefny, M., Abdel-Haleem, F., &ahmed, N. (2024). Synthesis, and Characterization of Magnetic Nano-particles using Opuntia Extract, and its Applications in Wastewater Treatment. *Egyptian Journal of Chemistry*, *67*(8), 171-178. doi: 10.21608/ejchem.2023.210360.7959

[50] Salama, M., Abdo, A., Mousa, A., Shaheen, A., Elsayed, A., & Soliman, A. (2022). Morus Alba Leaf Extract-Based Biogenic Production of Silver Nanoparticles: Characterization, Antibacterial, and Antiviral Evaluation. *Egyptian Journal of Chemistry*, *65*(132), 605-615. doi: 10.21608/ejchem.2022.153506.6682

[51] Mohamed, A., &Hassabo, A. (2022). Modified Cellulose Acetate Membrane for Industrial Water Purification. Egyptian Journal of Chemistry, 65(131), 53-70. doi: 10.21608/ejchem.2022.147513.6393.